

We appreciate the comments obtained from Sarah Bradley and an anonymous referee and have revised the manuscript accordingly.

Here is our reply to the referees' comments in purple.

Anonymous Referee #1

Title: the west coast of Bohai Bay?

Answer: 'west' was replaced by 'central', please see line1.

Abstract: The shoreline retreat and advance rates are never reported and discussed in the main text. They just pop up here.

Answer: this part was deleted, the focus is now on the reconstruction of the Holocene sea level rise in Bohai Bay (line35-40).

L26. The rapid rise of the sea?

Answer: changed to 'rapid sea-level rise' (line 25)

Introduction: I suggest authors rewrite this section which is weakly organized. The structure had better come in an order of a brief review of related sea-level studies leading to specific scientific questions targeted by this study and finally the solution of this study.

Answer: we feel this is what we did: outline the specific interest of the area due to specific questions (broad shelf effect, far-field, high fluvial sediment supply) of sea-level science which are subsequently explained and referenced. These are key topics of sea level science which we address in our study. We agree that a sentence about our solution was missing – now added (lines 62-63), and a brief review of related sea-level studies were added in "Study area", please see line 81-87.

L33-38 is vague and basically makes no sense.

Answer: it is part of the motivation of the study. We feel it makes sense and should stay (line45-50).

L41-44. What's the link between these two issues and this study? I did not see they were further discussed.

Answer: We agree and have changed the discussion text (lines277-286) to be in line with the introduction (lines 51-59)

"allow approximating"? It would be clear to say far-field sites usually have a sea-level history similar to IESL. "affect the sea level by up to 10 m" is also an unclear description.

Answer: text changed (line 53-55)

Section 3.4. It is necessary to point out the radiocarbon testing lab to which the samples were sent. The IntCal13 is a dataset independent from Calib program. So, it is not "IntCal13 of Calib". L119, "attained from bulk organic samples"?

Answer: the dating lab has been added (line 126-128) and Intcal13 separated from software (line 131)

L122: Change to "To develop SLIPs, salt-marsh:"

Answer: done (line 138)

L126-128. This sentence is too complicated to follow.

Answer: agreed and changed accordingly (lines 142-143)

L152-176. Why not set an independent section talking about lithostratigraphy?

Answer: Done, it is now summarised in section 4.1 and listed in Table S2

L166. Holocene maximum transgression limit?

Answer: yes and changed (line 182).

L169-172 is hard to follow.

Answer: We tried hard to comprehend this comment. We may well be blind but we did not find where the text lacks clarity.

Section 4.2 provides limited information of the SLIPs, which need detailed explanation combined with the lithostratigraphy, facies and foram results. More importantly, the reasons why they are chosen and what indicative meaning they are assigned should be given one by one. I suggest reorganizing Section 4. The modern analogue and indicative meaning can be put into new section 4.1. While the lithostratigraphy and SLIPs can be grouped in section 4.2. The comparison of reconstructed and modeled sea-level histories can be moved into the discussion.

Answer: Thank you, yes it was necessary to re-organise the Result section, now done in (1) lithostratigraphy and facies, (2) Foraminifera data (3) Modern analogue and indicative meaning and range, (4) SLIPs.

L182. There are plus symbols before elevations, so the “above” is redundant.

Answer: done, please see line 209.

L221. I have a doubt about making the sample with a date of 9718 cal. a BP in core Q7 as a SLIP. This could be biased by the old carbon effect.

In this section, authors need to compare their results with qualified sea-level records from other far-field regions, which were at a much lower height possibly below -25 m in 9700 cal. a BP.

Answer: Thank you, this is indeed an important point! We have revised the text accordingly (lines 264-273).

Not to mention that the SLIPs from this study have not been calibrated to remove the significant tectonic subsidence.

Answer: Yes, because we wanted to quantify the non-GIA component.

This conclusion is nearly void.

Answer: we understand that the referee has different expectations. We have now added the important point about the early Holocene shoreline elevation, please see line302-304 – thank you again for pointing this out to us.

Figure 1a should be zoomed out to display the entire East China Sea shelf, which also needs a label. Currently, it is similar to figure 1b.

Answer: Fig.1a has been zoomed out follow this comment

Figure 5. What does the bar chart mean? If the authors want to keep it, it deserves a name like “E”. The caption missed the transect A. In addition, please also keep a uniform format for the names of sub-figures. All in upper case or lower case.

Answer: the Fig. has been reorganized and rewritten, and the bar chart has been deleted.

Figure 7. Age error bars should be plotted for each SLIP.

Answer: age error bars were included in the plot - they are small. A note is now added to the caption.

Sarah Bradley, Referee #2

Missing information:

I am not sure if the paper is supposed to have SOM material - as it was not uploaded with the main manuscript, but I found a version within the uploaded earlier version.

Answer: Our paper is supposed to have supplement material and we apologise for its missing. The SLIP data on the graph are from Lambeck et al. 2014 data compilation. These data indicate a small (~0.5m) highstand at 7-6 ka occurring the south of Bohai Bay. The data do confirm the Bradley et al model prediction (Bradley et al 2016).

In this document:

(i) what are the SLIP data on the graph? Is this different from the record in the paper? It is from a latitude of 33-37N.

Answer: yes, the SLIP data in Fig. S3 are from latitude 33-37N.

(ii) Table: the Bradley model is not shown but is referenced in the paper and is missing. Given this information, I am reviewing the paper without using this information.

Answer: We are not sure what you mean with “the Bradley model... is missing” – it is correct that we haven’t shown the model result because we don’t have the data, but we compared our results with those published in Bradley et al 2016 (Fig. 12, BB)

Abstract:

There is discussion in the abstract about information that is not provided in the paper: Line 26-30. This reads as a similar to the discussion and results in the Wang, 2015. I would suggest either revising the abstract to be related to what is presented in the paper or adding more work to the paper.

Answer: agreed and abstract text changed (line 35-40).

Introduction:

I would like the authors to provide an overview on the character of the Holocene sea level across China. As Zong, 2004 (given in the paper) has previously published, there is only a very minor highstand recorded at the other sites across the region. It is therefore important to put your new SLIP record into this context. A SLIP record which does not record a large highstand, as the authors have found is not unusual for the region. The authors do reference some other material, but as I state below it is not in English so unfortunately is not accessible by the wider scientific community to which ESD is aimed.

Answer: a paragraph describing the SLIPs is now added in ‘Supplement file’, and a brief introduction of previous studies were also added in “Introduction”(line 55-58) and “The study area” (lines81-87).

Page 3: line 70: ‘During the Holocene the sea inundated the coastal area with the shoreline moving 80 km inland’ (Wang et al., 2015). Can you state how this was determined?

Answer: It was determined through the identification of marine layers and their respective elevation. We feel it is not necessary at this point to outline the ‘how determined’

From briefly looking at this paper, it describes three of the cores described in this paper. Is this new study a follow on from this?

Answer: yes.

Page 3: line 71: Over 130 SLIPs established for the past 6000 calendar years (Li et al., 2015) Are the authors referring to another study from this region that has already published 130 SLIP? Where are these from? Are they relevant to the paper? If there are 130 extra points from this region - they should be included within this study as this paper is referred to through the study.

Answer: we agree that mentioning Li et al without showing the data points creates confusion. We have now added a paragraph in 'The study area' where the SLIPS are described. In addition, the 136 SLIPs are now displayed in Fig. S2 and the SLIP research in the area is outlined in a supplement paragraph which includes Fig. S1.

References:

The authors refer to a number of papers to give support to their statements in the paper (for example, Li et al., 2015 (as listed above)). Unfortunately as these publications are not in English they are not likely to be accessible to the wider scientific audience. It would be useful if they authors can elaborate at least the method in the papers which the statements they use are based.

Answer: see above

GIA modelling+ Residual: method

Fig7: List the earth model used in the figure caption.

Answer: done, please see the caption of Fig. 7.

Page 29: line 507: 'interpolated model data points'. Do the authors use just the RSL prediction to take the residual, rather than generating a RSL at the exact location and time of each SLIP?

Answer: we have generated RSL curves for a single point that is representative of all the locations. Plotting one curve for each location would give a set of indistinguishable curves, due to inherent long-wavelength character of GIA. Regarding time, we have computed RSL on a grid of time points spaced by 500 years and obtained the RSL predictions at the exact time of each SLIP through linear interpolation.

The authors have looked into the sensitivity to the ice sheet model in the GIA- but using two different ice sheet reconstruction in the generation of the predictions; ICE6G and ANU, which have very different end to the timing of global melting. However I am surprising that this makes so little difference to the resultant RSL predictions?

Answer: yes indeed, the models have different histories of melting, but they employ also different lower mantle viscosities. The two models (ICE, ANU) have been developed independently and it is good to see that, at least for our study site, they converge towards a common set of RSL predictions.

can the authors comment on this

(ii) On Page 6: line 138: 'Intrinsic uncertainties are estimated from GIA predictions with the models listed above'. This is not the case and the results do not support this statement, The authors do not consider the uncertainty to earth model.

Answer: Thank you for pointing this out. There was a misunderstanding between authors about model uncertainties because the difference between independent model results does reflect model uncertainty, although qualitatively only. We have now deleted the sentence (line 159-160).

They reference in the paper, that Bradley et al. 2016 examined a range of earth model and concluded a very different range of earth model parameters were required to resolve the large overprediction to the SLIP data. I am not stating that this is the correct model to use. However, a some of the ~ 5m overprediction to the SLIP data could be due to inaccurate model parameters. This needs to be considered to support the conclusion the authors draw regarding the rate of subsidence and geography evolution. As the results in the paper are based on determining the residual between the predicted RSL and the SLIP, this needs to be considered.

Answer: We understand these concerns. The Bradley et al study was not only part of a PhD research with corresponding resources but also based on >300 SLIP data. Our approach was different: scrutinising the SLIP data and employing “standard” GIA models. This, however, does not allow estimating input uncertainties. Carrying out a comprehensive analysis of model uncertainties associated with input model parameters would well be beyond the scope of this work, also in view of the limited dataset.

Section 4.2:

In this section the authors have calculated rates: Please state over which time interval this is for? 9- 6ka have a very different rate c.f 0-2ka. If the authors are calculating the rate from the data, how are they accounting for the errors?

Answer: We think that exact quantification of rates would be misleading. We used the ~ symbol for the rates and ‘early Holocene, ‘mid-late Holocene’ as time intervals. This is to describe the differences and offsets relative to each other within the time intervals which are very obvious from the plot in Fig 7a. We think discussing rough estimates of rates is valid here while (very large) error margins would blur the picture.

Section 5.3: Line 233=237. The results for BRAD model are not provided.

Answer: correct and agreed that the text is misleading. We have now separated the comparison between Slips and “our” GIA model results on one side and Slips and Brad model results on the other side (Table S1).

Line 242: ‘Because the misfit disappears in South of Bohai Bay’ ...the most obvious explanation is the subsidence of the coastal plain’. This is not a correct statement. The misfit does not appear. I do not disagree that some of this misfit is due to subsidence but with the evidence the authors have provided it is not possible to conclude all the misfits are related to this process.

Answer: yes, agreed and text changed (line 282-286)

Line 251: ‘... early Holocene dominated by global sea-level rise and associated GIA effects which in the mid-late Holocene it is dominated by combination of tectonic subsidence. The authors do not provide the information to support this statement.

Answer: The support is now provided through the comparison between Bohai Bay SLIPs and SLIPs south of the Bay (Fig. S3). We have also explained the geological structure of the area (lines 282-286).

There has been little discussion of the signal over the mid-late Holocene. What do the authors define as mid-late? (4-0ka?)

Answer: Yes, mid-late is around 4-0 ka (Walker et al 2012, JQS 27, 649).

The last sentence in section 5.3 (now lines 295-296) discusses the mid-late Holocene rise in comparison to the one in the early Holocene. This is indeed not much because we do not have high quality data for the last 2000 years.

Holocene sea-level change on the ~~west-central~~ coast of Bohai Bay, China

Fu Wang^{1,2}, Yongqiang Zong³, Barbara Mauz^{4,5}, Jianfen Li^{1,2}, Jing Fang⁶, Lizhu Tian^{1,2},
Yongsheng Chen^{1,2}, Zhiwen Shang^{1,2}, Xingyu Jiang^{1,2}, Giorgio Spada⁷ and Daniele Melini⁸

¹Tianjin Center of Geological Survey, China Geological Survey (CGS), Tianjin, China

²Key Laboratory of Coast Geo-Environment, China Geological Survey, CGS, Tianjin, China

³Department of Earth Sciences, The University of Hong Kong, Hong Kong SAR, China

⁴School of Environmental Sciences, University of Liverpool, Liverpool, UK

⁵Department of Geography and Geology, University of Salzburg, Salzburg, Austria

⁶College of Urban and Environmental Science, Tianjin Normal University, Tianjin, China

⁷Department of Science, University of Urbino, Urbino, Italy

⁸Istituto Nazionale di Geofisica e Vulcanologia, Roma, Italy

Correspondence to: Fu Wang (wfu@cgs.cn)

Abstract. To constrain models on global sea-level change regional proxy data on coastal change are indispensable. Here, we reconstruct the Holocene sea-level history of the northernmost ~~East~~ China Sea shelf. This region is of great interest owing to its apparent far-field position during the late Quaternary, its broad shelf and its enormous sediment load supplied by the Yellow River. This study generated 25 sea-level index points for the central Bohai coastal plain through collected the study of 15 sediment cores and their sedimentary facies, foraminiferal assemblages and radiocarbon dating from the coastal plain of west Bohai Bay and extracted 25 sea level index points through the analyses of the basal peat, sedimentary facies, foraminiferal assemblages and radiocarbon dating. The observational data were compared with sea-level predictions obtained from global GIA models and with published sea-level data from Sunda shelf, Tahiti and Barbados. ~~The~~ Our observational ~~data se proxy data~~ indicate a phase of rapid sea-level rise from c. -17 m to -4 m ~~of mean sea level~~ between c. 10 ka and ~~6.5 ka~~ with, which includes a rapid peak rise of 6.4 mm/a during 8.7 ka to 7.5 ka and slower rise of 1.9 mm/a during 7.5 ka to 5.3 ka. ~~This was~~ followed by a phase of slow rise from ~~6.5 ka to 2 ka~~ (~0.4 mm/a from -3.58 m of 5.3 ka cal BP to -2.15 m of 2.3 ka cal BP). ~~In contrast to previous studies our data suggest~~

29 ~~that the sea level remained c. 2.5–1 m below the modern mean sea level during the mid-late Holocene. The~~
30 ~~comparison difference with between proxy data and the~~ sea-level predictions ~~for the study area and the~~
31 ~~published sea-level data is insightful; in the early Holocene Bohai Bay's sea-level rise is dominated by a~~
32 ~~combination of the eustatic and the water load components causing the levering of the broad shelf. In the mid-~~
33 ~~late Holocene the rise is dominated by a combination of tectonic subsidence and fluvial sediment load based~~
34 ~~on three GIA models suggests that the Bohai coastal plain experiences subsidence at a rate of around 1.25~~
35 ~~mm/a since about 7 ka~~ which masks the mid-Holocene highstand recorded elsewhere in the region. ~~Thus,~~
36 ~~during the early Holocene rapid rise the sea flooded the coastal plain and the shoreline retreated landwards at~~
37 ~~a rate of c. 40 m/a. It stayed at the landward maximum marine limit during the mid-Holocene when the sea-~~
38 ~~level rise slowed down allowing vertical sedimentary accretion to occur in the landward areas. During the late~~
39 ~~Holocene fluvial sediment supply outpaced the sea-level change and the shoreline prograded seawards at a rate~~
40 ~~between 20 and 10 m/a.~~

41

42

43 KEYWORDS: Sea level; Holocene; Glacial Isostatic Adjustment; Ice Equivalent Sea Level; Bohai Bay

44 1. Introduction

45 The sea-level rise since the mid-19th century is one of the major challenges to humanity of the 21st century
46 (IPCC, 2014). The driving mechanisms of this rise are relatively well-known on a global scale, but on a
47 regional scale the mechanisms are modified by local parameters. One of these parameters is the regional
48 Holocene sea-level history, which is a background sea-level signal of variable amplitude. In fact, the regional
49 response to sea-level changes may be very different from the global signal (Nicholls and Cazenave, 2010),
50 and, understanding regional coastal environment is a rising demand of policy makers. Here, we study the
51 Holocene sea-level history of Bohai Sea, which is the northernmost part of ~~the YellowChina~~ Sea. The area is
52 of special interest because its shoreline is situated on the broad shelf of the East China Sea (Fig. 1) in the far-
53 field of the former ice sheets. While the far-field site should have a sea-level history similar to the ice-

54 equivalent sea level, the broad shelf is thought to affect the sea-level by up to 10 m height (e.g. Milne and
55 Mitrovica, 2008) in a spatially complex manner. For example, only a very minor Holocene highstand was
56 recorded at sites along the southeast and south coast of China (Zong, 2004). In fact, no obvious Holocene
57 highstand was recorded in the Hangzhou Bay (Xiong et al., 2020) and the Pearl River delta (Xiong et al.,
58 2018). In addition, the exceptionally high supply of fine-grained fluvial sediment to the bay should have
59 influenced shoreline migration in the past. In order to reliably constrain the sea-level history in such complex
60 settings, high-resolution proxy data are required and compared with glacio-isostatic adjustment (GIA) model
61 predictions where the difference between model and proxy datum should allow inferring the non-GIA, hence
62 local, impact on the sea-level history. We show here that shelf effect and local processes influence the
63 regional sea-level history at different times.

64 **2. The study area**

65 The study area lies in a mid-latitude, temperate climate zone (Fig. 1a) on the north-western coast of the East
66 China Sea's wide shelf. Geologically, the Bohai Bay is a depression filled by several kilometre-thick
67 Cenozoic sediment sequences with the top 500 m ascribed to the Quaternary (Wang and Li, 1983). The long-
68 term tectonic subsidence has been estimated to about 1.3-2.0 mm/a at Tianjin City (Wang et al., 2003). The
69 Bay is a semi-enclosed marine environment, connected to the Pacific through a gap between the two
70 peninsulas, Liaodong Peninsulas and Shangdong Peninsulas and the Yellow Sea (Fig. 1b). Our study area is
71 the central coast of the Bay which lies between two deltaic plains, the Yellow River delta in the south and the
72 Luan River delta in the north (Fig. 1b). Several small rivers (e.g., Haihe and Duliujianhe, Fig. 1c) cut through
73 the coastal plain and enter the Bay. The coastal lowland is characterised not only by its low-lying nature,
74 (less than 10 m above sea level), but also by a series of Chenier-chenier ridges situated south of the Haihe
75 River and buried oyster reefs situated north of the Haihe River (Fig. 1c; Li et al., 2007; Su et al., 2011; Wang
76 et al., 2011; Qin et al., 2017). Local reference tidal levels such as mean high waters (MHW) and highest high
77 waters (HHW) are 1.25 m and 2.30 m respectively, based on the four tidal stations on the ~~west~~ coast of Bohai
78 Bay (Fig. 1c). During the Last Glacial Maximum the shoreline moved to the shelf break of the Yellow Sea,

79 more than 1000 km to the east and southeast of our study area (e.g., He, 2006). During the Holocene the sea
80 inundated the coastal area with the shoreline moving about 80 km inland (e.g., Wang et al., 2015).
81 Previous studies focused on the chenier ridges and palaeo-shoreline change of Bohai Bay (Wang, 1964).
82 Subsequently, a series of studies on marine transgression and lithostratigraphy provided the framework for
83 understanding the late Quaternary evolution of Bohai Bay (e.g., Zhao et al., 1979; Fig. S1). Over 130 Holocene
84 sea-level data, generated in the study area since the early 60ths, were recently compiled by Li et al. (2015; Fig.
85 S2; for details see supplement). However, because no correction for compaction was carried out and no
86 screening took place by which unsuitable material (e.g., transported shell) is rejected, the dataset requires
87 further scrutiny and is not used in our study.

88 **3 Methods**

89 **3.1 Sampling and elevation measurements**

90 To obtain sedimentary sequences for this study, we consulted previous studies (e.g. Cang *et al.*, 1979; Geng,
91 1981; Wang *et al.*, 1981; Wang, 1982; Yang and Chen, 1985; Zhang *et al.*, 1989; Zhao *et al.*, 1978; Xue et
92 al., 1993) to learn where in the bay marine deposits are dominant and where the landward limit of the last
93 marine transgression should occur. We then collected 15 cores along W-E transects from the modern
94 shoreline to 80 km inland (Fig. 1c), using a rotary drilling corer. Transect A, comprising 6 cores, stretches
95 from the modern shoreline 80 km inland and crosses the inferred Holocene transgression limit (Xue, 1993).
96 Transects B, C and D, comprising 9 cores, cross the transgression limit a little further south (Fig. 1c). The
97 surface elevations of the drilled cores were levelled to the National Yellow Sea 85 datum (or mean sea level,
98 MSL) using a GPS-RTK system with a precision of 3 cm. The GPS-RTK raw data were corrected and
99 processed to National Yellow Sea 85 datum system by the CORS system network available from the Hebei
100 Institute of Surveying and Mapping with National measurement qualification.

101 **3.2 Sediment and peat analyses**

102 In the laboratory, the sediment cores were opened, photographed and recorded for sedimentary characteristics
103 including grain size, colour, physical sedimentary structures, and content of organic material. To study the

104 degree of marine influence in the muddy sediment sequences, sub-samples were collected in 20 cm intervals.
105 These were analysed with respect to diatoms and foraminifera with a subsequent focus on the foraminifera
106 due to poor preservation of diatoms. The foraminifera of the $>63\mu\text{m}$ fraction of 20 g dry sample were
107 counted (e.g., Wang et al., 1985) following studies on modern foraminifera (e.g. Li, 1985; Li et al., 2009).
108 Sediment description followed Shennan et al. (2015): where in the sediment sequences foraminifera first
109 appear and/or significantly increase (from zero or less than 10 to more than 50) is noted as transgressive
110 contact, while the sediment horizon where foraminifera disappear and/or decrease significantly are noted as
111 regressive contact. These changes are often associated with lithological changes, such as from salt-marsh
112 peaty sediment to estuarine sandy sediment or tidal muddy sediment across a transgressive contact, or vice
113 versa. In addition, peat material was analysed in terms of its foraminifera content so that salt-marsh peat can
114 be differentiated from freshwater peat.

115 3.3 Analysis of compaction

116 Because the Holocene marine deposits are mainly unconsolidated clayey silt with around 0.74% organic
117 matter (Wang et al. 2015) post-depositional auto-compaction (Brain et al., 2015) may have led to lowering of
118 the SLIP. According to Feng et al. (1999), the water content and compaction of marine sediments show
119 positive correlation with the down-core reduction of water content of the Holocene marine sediment being
120 about 10%. Based on these observations, we assumed the maximum lowering is about 10% of the total
121 thickness of the compressible sediment beneath each SLIP. Consequently, the total lowering for an affected
122 SLIP is 10% of the total thickness of the compressible sequence beneath the dated layer divided by the post-
123 depositional lapse time proportional to the past 9000 years (e.g. Xiong et al., 2018), i.e. since the marine
124 transgression in the study area.

125 3.4 Radiocarbon analyses

126 69 bulk organic sediment samples from salt-marsh peat were collected from drilling cores, and the peat or
127 plant subsamples obtained from these bulk sediments were chosen for AMS radiocarbon analysis at Beta
128 Analytic Inc. because these can give more reliable ages than shells for the SLIPs. The resulting raw

129 radiocarbon ages were converted to conventional ages after isotopic fractionation were corrected based on
130 $\delta^{13}\text{C}$ results. The conventional radiocarbon ages were calibrated to calendar years using the data set Intcal13
131 [included in the software](#) Calib Rev 7.0.2 for organic samples, peat and plant samples (Reimer, *et al.*, 2013).
132 Because Shang *et al.* (2018) reported age overestimation of 467 years for the bulk organic fraction of salt-
133 marsh peaty clay compared to the corresponding peat fraction, all the AMS ^{14}C ages between 4000 to 9000
134 BP obtained from salt-marsh samples were corrected by $Y=0.99X-466.5$ (Y is the corrected age, X is the age
135 obtained from the organic fractions; Shang *et al.*, 2018) except one <600 years age from borehole Q7 (Table
136 1).

137 3.5 Sea-level index points (SLIPs)

138 [To develop](#) SLIPs, salt-marsh peaty clay layers were used. To convert the dated peat layers into a SLIP, the
139 modern analogue approach was used by measuring the elevation of the modern open tidal flat (Fig. 2) and
140 sampling its surface for their foraminiferal content. Following the studies of the modern foraminifera
141 assemblage (Li, 2009) *Ammonia beccarii* typically occurs in the upper part of an intertidal zone and
142 *Elphidium simplex* in the lower intertidal zone. The [zonation of the modern](#) foraminifera assemblage [was](#)
143 [then used to identify](#) the [indicative meaning of the](#) salt-marsh peat layers: the paleo-mean sea level is the
144 midpoint between high water of spring tides (HHW:+2.3 m) and mean high waters (MHW:+1.25 m) which is
145 1.78 m with ± 0.53 m uncertainty (Wang *et al.*, 2012, 2013; Li *et al.*, 2015). For each dated salt-marsh peat
146 layer the indicative meaning and range, the total amount of possible lowering in elevation due to sediment
147 compaction and the reconstructed elevation of palaeo-MSL are listed in Table 1.

148 3.6 GIA modelling

149 The time-evolution of sea level was obtained using the open source program SELEN (Spada and Stocchi,
150 2007) to solve the "Sea Level Equation" (SLE) in the standard form proposed in the seminal work of Farrell
151 and Clark (1976). In its most recent development, SELEN (version 4) solves a generalized SLE that accounts
152 for the horizontal migration of the shoreline in response to sea-level rise, for the transition from grounded to
153 floating ice and for Earth's rotational feedback on sea level (Spada and Melini, 2019). The programme
154 combines the two basic elements of GIA modelling (Earth's rheological profile and ice melting history since

155 the Last Glacial Maximum) assuming a Maxwell viscoelastic incompressible rheology. The GIA models
156 adopted are ICE-5G(VM2) (Peltier et al., 2004), ICE-6G(VM5a) (Peltier et al., 2012), both available on the
157 home page of WR Peltier, and the one developed by Kurt Lambeck and colleagues (National Australian
158 University, denoted as ANU hereafter; Nakada and Lambeck, 1987, Lambeck et al., 2003) provided to us by
159 A Purcell (pers. com. 2016). ~~Intrinsic uncertainties are estimated from the comparison of GIA predictions~~
160 ~~obtained with the models listed above (Melini and Spada, 2019).~~ Table S1 summarises the values used for
161 each model. The palaeo-topography has been solved iteratively, using the present-day global relief given by
162 model ETOPO1 (Amante and Eakins, 2009). All the fields have been expanded to harmonic degree 512, on
163 an equal-area icosahedron-based grid (Tegmark, 1996) with a uniform resolution of ~20 km. The rotational
164 effect on sea-level change has been taken into account by adopting the “revised rotational theory” (Mitrovica
165 ~~and Wahr and Mitrovica~~, 2011).

166 4. Results

167 4.1 Lithostratigraphy and facies

168 Lithostratigraphically, the cores show a succession of terrigenous (including fresh-water swamp, river
169 channel, flood plain), salt-marsh and marine sediments (Table S2) with a clear W-E trend from terrestrial to
170 marine dominance of deposits (Fig. 3-6). The around 80 km long transect A shows this trend: close to the
171 modern shoreline pre-Holocene terrigenous sediments are overlain by basal peat including salt-marsh peat or
172 peaty clay. Further inland these are replaced by fresh-water peat overlain by salt marsh and intertidal
173 sediments and, above, by terrigenous sediments. The cores DC01, CZ01 and CZ02 are composed of fluvial
174 sediments only, roughly confirming the Holocene maximum transgression inferred by Xue (1993). Multiple
175 shifts between salt marsh, marine and fluvial deposits are noticeable in cores QX02, QX03, CZ61 which
176 originate from the central part of the study area.

177 Marsh deposits are either a blackish and thin freshwater peat mostly interbedded in yellowish fluvial
178 sediments or a yellowish-brown salt-marsh peat bearing intertidal foraminifera (Table 1). Their lower
179 boundaries are usually sharp, and their upper boundaries are mostly diffused or the salt-marsh peat changes
180 gradually into dark grey intertidal sediments. Salt-marsh peat is intercalated in marine sediment sequences
181 (i.e. QX01, QX02, CZ61, CZ85, CZ66 and CZ03, Fig. 3-6), particularly at sites that are close to the
182 Holocene maximum ~~landward~~ transgression limit.

4.2 Foraminifera data

Foraminifera were identified in all cores except CZ01, CZ02 and DC01 which originate from the landward site of the maximum transgression limit. As the Fig. 4 and 6 show that, foraminifera start to appear at 11.2 m depth, which is dated to about 7.85 ka cal BP in QX01. Abundance of fossil foraminifera changes from about 404 – 772 individuals per samples at depths from 11.2 m to 10.8 m, 68 – 338 specimens from 9.4 m to 8.8 m, and 103 – 3456 counts from 8.2 m to 7.6 m. The assemblages reach maximum abundance at 6.6 m depth which is dated to between 5.29 and 5.23 ka cal BP, with over 30,000 individuals per sample, before disappearing at 5.6 m. Dominant species change from *Nonion glabrum* in 11.2 – 7.4 m to *Ammonia beccarii* vars. in 7.4 – 6.4 m. This change represents a change from a salt-marsh to a lagoon. In QX02, the pattern of foraminifera distributions is very similar. Low numbers of foraminifera, mostly *Nonion glabrum*, start to appear at about 10.1 m (-6.53 m of sea level), as dated to between 7.87 and 7.49 ka cal BP. The abundance reaches its highest at 6.7 m (-3.13 m of sea level), and the assemblages were dominated by *Ammonia beccarii* vars. Foraminifera disappears sometime between 5.72 and 3.52 ka cal BP. In all seaward drilling core, CZ03, CZ80, CZ85, CZ66, CZ87, CZ61, CZ65, ZW15 and Q7, the pattern of foraminifer's distributions are very similar as QX01 and QX02 (Fig. 4). The foraminifera start to appear in low numbers in the layer just above the basal peaty clay. This first appearance is in ca. 17-8 m depth dated to 9-7 ka cal BP. Above this depth the count increases from ~100 to ~3000 foraminifera per sample at ca 8-7 m depth. The maximum count with >30,000 individuals per sample is reached at -6-5 m dated to around 5 ka cal BP. Foraminifera disappear in these cores sometime between 5.7 ka cal BP and 3.5 ka cal BP. The foraminifera assemblage is composed of few species only, hence not rich and first dominated by *Nonion glabrum* in 17-7 m depth and then dominated by *Ammonia beccarii* vars. in 7-6 m depth. Other species found are *Quinqueloculina akneriana rotunda* and *Protelphidium tuberculatum* (Figs. 4 and 6).

4.3 Modern analogue and indicative meaning and range

The data obtained from the modern analogue shows that the tidal flat can be divided into two sub-environments: intertidal with bioturbation (worm hole developed in tidal surface) and supratidal with salt-marsh vegetation (Fig. 2). Within the supratidal and salt-marsh zones, the foraminiferal assemblages are

209 dominated by *Ammonia beccarii* covering an elevation range from +1.42 m to +2.00 m ~~above msl~~, including
210 the +1.79m boundary of salt marsh with plants. At sites below these elevations, i.e. intertidal with
211 bioturbation (Fig. 2), the foraminiferal assemblages are dominated by *Elphidium simplex*, *Ammonia beccarii*
212 and *Pseudogyroidina Sinensis*. This foraminiferal zone covers an elevation ranging from 1.42 m to modern
213 MSL.

214 Besides occasional *A.beccarii* there are few living foraminifera in the salt marsh above the MHW. The
215 abundance is either biased towards *Ammonia beccarii* or it is relatively small. The latter is most probably due
216 to the area being situated above the MHW and, hence, subject to evaporation during low tide, with the
217 consequence of a relatively high and highly variable salt content of the pore water in the intertidal zone. The
218 modern analogue samples confirm the bias towards salt-tolerant species (Fig. 2, Table 1). The spatial
219 distribution of the ages confirms the E-W trend of the Holocene transgression where the oldest age is close to
220 the modern shoreline and the youngest age is close to the maximum transgression limit.

221 4.4 Sea-Level Index Points

222 In total 25 sea-level index points were established from the dated basal salt-marsh peat using the information
223 obtained from the modern analogue. In Core Q7, at the most seaward location in the study area, the basal
224 SLIP is dated to ~9700 cal BP (Table 1), marking the onset of marine inundation of the study area. The
225 overlying marine sequence is capped by a thick layer of shelly gravels at 1.30 m depth and the associated
226 SLIP is dated to 540 cal BP. This marks the upper end of the marine sequence as foraminifera start to
227 disappear alongside a change from intertidal to supratidal environmental conditions. The cores ZW15, QX02,
228 QX03, QX01 show the same sequence as Q7 and provide 6 SLIPs. 19 SLIPs were collected from other cores
229 (Table 1).

230 3. Discussion

231 5.1 Quality of SLIP data

232 Owing to elevated and variable salinity of the coastal water samples from both cores and modern tidal flat are
233 characterised by low microfauna diversity and low number of foraminifera species. This precludes the use of
234 transfer function statistics and compels analysis based on direct comparison with the modern environment.

235 We have solved this analytical problem by establishing SLIPs exclusively from basal salt-marsh peat in
236 transgressive contact and by correcting the data for compaction. This analytical rigor allowed generating
237 more accurate and more precise SLIP data than those reported by Li et al. (2015) because these earlier SLIP
238 data are characterised by relatively poor chronological and elevation control (for details see supplement).

239 Notwithstanding SLIP improvement in terms of accuracy and precision, fluctuation of the data exist that can
240 exceed 1 m (e.g. at 3.9 ka and at 5.2 ka, Fig. 7). Although hard to prove due to lack of data, we believe that
241 these fluctuations are caused by groundwater extraction which lowers the surface in places.

242 5.2 The observed Holocene sea-level rise

243 The SLIPs established indicate two phases of sea-level rise during the Holocene. The first phase occurred in
244 the early Holocene until ~6.5 ka when the sea level rose from -17 m to -4 m. The second phase occurred from
245 ~6.5 ka to 2 ka when the sea level rose from -4 m to -2 m. The oldest Holocene shoreline in Bohai Bay is,
246 situated at -17.2 m at ~9,700-7 ka cal BP, similar to Tian et al. (2017) who indicate ~-20 m at 9.4 ka cal BP
247 based on seismic units and drilling cores. Between around 8.8 ka and 7.5 ka cal BP the sea level rose rapidly
248 from -15.4 m to -7.0 m at a rate of ca 6.4 mm/a. Then, from 7.5 ka to 5.2 ka cal BP the relative sea level rose
249 to -3.6 m at an average rate of 1.9 mm/a and to -1.2 m until 3.8 ka cal BP, before falling to -2.1 m at 2.3 ka
250 cal BP with an average rising rate of ca. 0.4mm/a from 5.2 to 2.3 ka cal BP. The final phase from 2 ka to
251 today is constrained by only one SLLP from core Q7 dated to 540 cal BP at ~0.5 m (Table 1).

252 Lithostratigraphic data (Shang et al., 2016) suggest that surface of the intertidal sediment body remained very
253 close to zero m from the landward limit of the marine transgression to about 2 km inland from the present
254 shoreline. Further inland, in borehole ZW15 the surface elevation of the same intertidal sediment body is

255 ~3.0 m lower than in core Q7 (Figs. 3 and 4) suggesting a rise of sea level in Bohai Bay in the last 1000
256 years.

257 5.3 Observed and predicted Holocene sea level

258 We compare our observational data with GIA models employed in this study and with Bradley et al. (2016;
259 henceforth denoted as BRAD; see also Table S1) who examined several ice-melting scenarios together with a
260 range of Earth-model parameters, and validated model outputs using published SLIP data from East China
261 Sea coast including Bohai Bay.

262 Figure 7a displays observational data and sea-level predictions generated in this study. It shows that none of
263 GIA models approximates the observations. The difference ranges between around 14 m at 9 ka and 3 m at
264 2.5 ka. Bohai Bay's oldest Holocene shoreline (~9.7 ka cal BP) is at -17.2 m (observed), at ca – 35 m (ANU)
265 or at ca -10 m (ICE-X). The BRAD model predicts this shoreline to be at ~-20 m at 10 ka. Our observed
266 shoreline elevation is similar to Sunda Shelf (ca -15 m; Hanebuth et al., 2011) but different to the islands of
267 Tahiti (ca -28 m; Bard et al., 2010) and Barbados (ca -25 m; Peltier and Fairbanks, 2006). There are two
268 ways to interpret this: (i) the age of the lowermost SLIP in core Q7 is overestimated due to old carbon
269 contamination of the dating material or, (ii) the relatively shallow shoreline position in our study area is a
270 deviation from eustacy due to levering of the broad continental shelf in response to ocean load (e.g., Milne
271 and Mitrovica, 2008). The similarity to the Sunda Shelf and absence of contamination elsewhere in the
272 sediment cores suggests indeed that the broad-shelf effect (East China Sea shelf; Fig. 1) causes the shallow
273 shoreline position. More SLIP data are needed to ~~but our study does not provide unequivocal evidence for it.~~

274 While SLIP data suggest a rising rate of ~0.4 cm/a during the early Holocene, the GIA models indicate ~0.5
275 cm/a (ICE-X) and ~0.9 cm/a (ANU). The ICE-X models approximate the observed early Holocene rising rate
276 but the timing of this rise is offset by about 2000 years. In the ANU model the early Holocene sea level rises
277 almost twice as fast as the observed one with an offset of ~500 years. Thus, the observed early Holocene sea
278 level rises slower than the modelled sea level. For the mid-late Holocene SLIP data suggest ~0.04 cm/a rising
279 rate while the GIA models indicate a falling sea level. Predictions obtained from ICE-5G and ICE-6G are

280 generally relatively similar but deviate from each other in the timing of the mid-Holocene sea-level
281 highstand. The GIA models, including BRAD, show the highstand (4.6 m -3.4 m; 0.5 m) at 7-6 ka while the
282 SLIP data remain below modern sea level until 2 ka. The misfit between observed and predicted sea level rise
283 is in the coastal zone south of Bohai Bay much smaller than in our study area (Fig. S3). This should reflect
284 the geological structure of the area: our study area belongs to the North China Plain Subsidence Basin (Wang
285 and Li, 1983), while the south of Bohai Bay lies on the edge of Shandong Upland (Fig. 1b). Thus, the most -
286 likely explanation for the Bohai Bay misfit is subsidence of the coastal plain. Subsidence is a non-GIA
287 component and should become evident through the residuals (i.e. the difference between observation and
288 prediction per unit of time; Fig. 7b). Indeed, we identify linearity of residuals for the period 7-0 ka,
289 suggesting that subsidence dominates the local sea-level signal after the rise of the eustatic sea level has
290 slowed down. A subsidence rate of 1.25 mm/a is estimated from the residuals, similar to Wang et al. (2003)
291 who deduced a rate of ~1.5 mm/a from the 400-500 m thick Quaternary sequence in the bay. It is possible
292 that fluvial sediment supply enhanced the subsidence rate in the Holocene. The Yellow River's annual
293 discharge into Bohai Bay is estimated to 0.2 Gt until 740AD rising to 1.2 Gt until around 1800 when
294 widespread farming on the loess plateau started increasing the river's sediment load (Best, 2019). Thus, the
295 sea-level rise in Bohai Bay is in the early Holocene dominated by the eustatic sea-level rise and GIA effects_
296 associated with the broad shelf from Bohai Sea to East China Sea, while in the mid-late Holocene it is
297 dominated by a combination of tectonic subsidence and fluvial sediment load.

298 4. Conclusions

299 Using advanced methods for field survey and identification of accurate and precise sea-level markers, we
300 have established a new Holocene sea-level history for central Bohai Bay. Our new data are not only different
301 to previously published data in that they do not show the expected mid-Holocene sea level highstand, but
302 they are also different to global GIA models. We see a possible broad-shelf effect elevating the shoreline by
303 several meters in comparison to the tropical islands of Tahiti and Barbados and we see local processes
304 controlling shoreline migration and coast evolution as soon as ice melting ceased. This indicates that more

305 emphasis should be placed on regional coast and sea-level change modelling under a global sea-level rising
306 future as the local government need more specific and effective advice to deal with coastal flooding.

307 5. ACKNOWLEDGMENTS

308 We thank one anonymous reviewer and Sarah Bradley for constructive suggestions on the manuscript. This
309 work was supported by the China Geological Survey, CGS (DD20189506) and National Natural Science
310 Foundation of China (Grant no. 41476074, 41806109, 41972196). The authors acknowledge PALSEA, a
311 working group of the International Union for Quaternary Sciences (INQUA) and Past Global Changes
312 (PAGES), which in turn received support from the Swiss Academy of Sciences and the Chinese Academy of
313 Science.

314 References

- 315 Amante, C. and Eakins, B.: ETOPO1 Arc-Minute Global Relief Model: Procedures, Data Source and
316 Analysis. Tech. rep, DOI: 10.7289/V5C8276M, 2009.
- 317 ~~Bard, E., Hamelin, B., Arnold, M., Montaggioni, L., Cabioch, G., Faure, G., Rougerie, F.: Deglacial sea-level~~
318 ~~record from Tahiti corals and the timing of global meltwater discharge. Nature, 382, 241–244.~~
319 ~~<https://doi.org/10.1038/382241a0>, 1996.~~
- 320 Bard, E., Hamelin, B. and Delanghe-Sabatier, D.: Deglacial meltwater pulse 1B and Younger Dryas sea
321 levels revisited with boreholes at Tahiti. Science, 327, 1235–1237. DOI: 10.1126/science.1180557, 2010.
- 322 Best, J.: Anthropogenic stresses on the world’s big rivers. Nature Geoscience, 12, 7–21.
323 Doi:10.1038/s41561-018-0262-x, 2019.
- 324 Bradley, S.L., Milne, G.A., Horton, B.P., Zong, Y.Q.: Modelling sea level data from China and Malay-
325 Thailand to estimate Holocene ice-volume equivalent sea level change. Quaternary Science Reviews, 137,
326 54–68. DOI: 10.1016/j.quascirev.2016.02.002, 2016.
- 327 Brain, M.J. Chapter 30 Compaction. In: Shennan, I., Long, A.J., Horton, B.P. (Eds.): Handbook of Sea-level
328 Research. John Wiley & Sons Ltd. Chichester, UK, 2015.

- 329 [Cang, S.X., Zhao, S.L., Zhang, H.C., Huang, Q.F.: Middle Pleistocene paleoecology, paleoclimatology and](#)
330 [paleogeography of the western coast of Bohai Gulf. Acta Palaeontologica Sinica 18\(6\): 579–591. DOI:](#)
331 [10.19800/j.cnki.aps.1979.06.006, 1979 \(in Chinese with English abstract\).](#)
- 332 Farrell, W. and Clark, J.: On postglacial sea-level. Geophys. J. Roy. Astr. S., 46, 647–667. DOI:
333 10.1111/j.1365-246X.1976.tb01252.x, 1976
- 334 Feng, X.L., Lin, L., Zhuang, Z.Y, Pan, S.C.: The relationship between geotechnical parameters and
335 sedimentary environment of soil layers since Holocene in modern Huanghe subaqueous Delta. Coastal
336 Engineering, 18, 4, 1–7. DOI: CNKI:SUN:HAGC.0.1999-04-000, 1999 (in Chinese with English abstract).
- 337 [Geng, X.S.: Marine transgressions and regressions in east China since late Pleistocene Epoch. Acta](#)
338 [Oceanologica Sinica, 3\(1\), 114–130.](#)
339 http://www.hyxb.org.cn/aos/ch/reader/create_pdf.aspx?file_no=19810110&flag=&journal_id=aos&year_id
340 [=1981, 1981 \(in Chinese with English abstract\).](#)
- 341 [Hanebuth, T.J.J., Voris, H.K., Yokoyama, Y., Saito, Y., Okuno, J.I.: Formation and fate of sedimentary](#)
342 [depocentres on Southeast Asia's Sunda Shelf over the past sea-level cycle and biogeographic implications.](#)
343 [Earth-Science Reviews, 104\(1–3\), 92–110. https://doi.org/10.1016/j.earscirev.2010.09.006, 2011.](#)
- 344 He, Q.X.(Eds.): Marine Sedimentary Geology of China. Beijing: China Ocean Press: 464–466, 2006 (in
345 Chinese).
- 346 IPCC: [Climate Change 2014: Synthesis Report. Contribution of Working Groups I, II and III to the Fifth](#)
347 [Assessment Report of the Intergovernmental Panel on Climate Change \[Core Writing Team, R.K. Pachauri](#)
348 [and L.A. Meyer \(eds.\)\]. IPCC, Geneva, Switzerland, 151 pp. https://www.ipcc.ch/report/ar5/syr/, 2014.](#)
- 349 Lambeck, K., Purcell, A., Johnston, P., Nakada, M., Yokoyama, Y.: Water-load definition in the glacio-
350 hydro-isostatic sea-level equation. Quaternary Science Reviews, 137, 54–68. DOI: 10.1016/s0277-
351 3791(02)00142–7, 2003.
- 352 [Li, J.F.; Kang, H.; Wang, H.; Pei, Y.D.: Modern geological action and discussion of influence factors on the](#)
353 [west coast of Bohai Bay, China. Geological Survey and Research, 30\(4\), 295–301.](#)

- 354 <http://www.tianjin.cgs.gov.cn/dzdcyyj/qkxz/20074/200801/P020160920812081540884.pdf>, 2007 (in
355 [Chinese with English abstract](#)).
- 356 Li, J., Pei, Y., Wang, F., Wang, H.: Distribution and environmental significance of living foraminiferal
357 assemblages and taphocoenose in Tianjin intertidal zone, the west coast of Bohai Bay. *Marine geology &*
358 *Quaternary geology*, 29(3), 9–21. DOI: CNKI:SUN:HYDZ.0.2009-03-004, 2009. (in Chinese with English
359 abstract).
- 360 Li, J., Shang, Z., Wang, F., Chen, Y., Tian, L., Jiang, X., Wang, H.: Holocene sea level change on the west
361 coast of the Bohai Bay. *Quaternary Sciences*, 35(2), 243–264. DOI: 10.11928/j.issn.1001-
362 7410.2015.02.01, 2015 (in Chinese with English abstract).
- 363 Li, S.L.: Distribution of the foraminiferal thanatocoenosis of PEARL River estuary. *Marine geology &*
364 *Quaternary Geology*, 5(2), 83–101. DOI: 10.16562/j.cnki.0256-1492.1985.02.009, 1985 (in Chinese with
365 English abstract).
- 366 [Milne, G.A. and Mitrovica J.X.: Searching for eustasy in deglacial sea-level histories. *Quaternary Science*](#)
367 [Reviews](#), 27, 2292–2302. DOI: 10.1016/j.quascirev.2008.08.018, 2008.
- 368 Mitrovica, J. and Wahr, J.: Ice Age Earth Rotation. *Annual Review of Earth and Planetary Sciences*, 39,
369 577–616. DOI: 10.1146/annurev-earth-040610-133404, 2011.
- 370 Nakada, M. and Lambeck, K.: Glacial rebound and relative sea-level variations: a new appraisal.
371 *Geophysical Journal International*, 90, 1, 171–224. DOI: 10.1111/j.1365-246X.1987.tb00680.x, 1987.
- 372 [Nicholls, R.J. and Cazenave A.: Sea-level rise and its impact on coastal zones. *Science*, 328, 1517–1520.](#)
373 [DOI: 10.1126/science.1185782, 2010.](#)
- 374 Peltier, W.R.: Global glacial isostasy and the surface of the ice-age Earth: the ICE-5G (VM2) Model and
375 GRACE, *Annu. Rev. Earth Pl. Sc.*, 32, 111–149.
376 <https://doi.org/10.1146/annurev.earth.32.082503.144359>, 2004.
- 377 Peltier, W.R., Drummond, R., and Roy, K.: Comment on Ocean mass from GRACE and glacial isostatic
378 adjustment by DP Chambers et al., *J. Geophys. Res.-Sol. Ea.*, 117, B11403.
379 <https://doi.org/10.1029/2011JB008967>, 2012.

- 380 [Peltier, W.R., and Fairbanks, R.G.: Global glacial ice volume and Last Glacial Maximum duration from an](#)
381 [extended Barbados sea level record, *Quat. Sci. Rev.*, 25\(23\), 3322–3337. DOI:](#)
382 [10.1016/j.quascirev.2006.04.010, 2006.](#)
- 383 [Qin, L., Shang, Z.W., Li, Y., Li, J.F.: Temporal and spatial distribution of the oyster reef in Biaokou to](#)
384 [Zengkouhe area; *Geological Survey and Research*, 40\(4\), 306–310.](#)
385 [http://www.tianjin.cgs.gov.cn/dzdcyyj/qkxz/20174/201802/P020180202566954723921.pdf, 2017 \(in](#)
386 [Chinese with English abstract\).](#)
- 387 Reimer, P.J., Bard, E., Bayliss, A., Beck, J.W., Blackwell, P.G., Ramsey, C.B., Buck, C.E., Cheng, H.,
388 Edwards, R.L., Friedrich, M., Grootes, P.M., Guilderson, T.P., Haflidason, H., Hajdas, I., Hatté, C.,
389 Heaton, T.J., Hogg, A.G., Hughen, K.A., Kaiser, K.F., Kromer, B., Manning, S.W., Niu, M., Reimer,
390 R.W., Richards, D.A., Scott, E.M., Southon, J.R., Turney, C.S.M., van der Plicht, J.: IntCal13 and
391 MARINE13 radiocarbon age calibration curves 0–50000 years cal BP. *Radiocarbon*, 55(4), 1869–1887.
392 doi: 10.2458/azu_js_rc.55.16947Bronk Ramsey C and Lee S (2013), 2013.
- 393 Shang, Z.W., Wang, F., Li, J.F., Marshall, W.A., Chen, Y.S., Jiang, X.Y., Tian, L.Z., Wang, H.: New
394 residence times of the Holocene reworked shells on the west coast of Bohai Bay, China. *Journal of Asian*
395 *Earth Sciences*, 115, 492–506. DOI: 10.1016/j.jseas.2015.10.008, 2016.
- 396 Shang, Z.W., Wang, F., Fang J., Li, J.F., Chen, Y.S., Jiang, X.Y., Tian, L.Z., Wang, H.: Radiocarbon ages of
397 different fractions of peat on coastal lowland of Bohai Bay: marine influence? *Journal of Oceanology and*
398 *Limnology*, <https://doi.org/10.1007/s00343-019-7091-7>, 2018.
- 399 Shennan, I., Long, A.J. and Horton, B.P.(Eds.): *Handbook of sea-level research*. Published by John Wiley &
400 Sons, Ltd., 2015.
- 401 Spada, G. and Stocchi, P.: SELEN: a Fortran 90 program for solving the “Sea Level Equation”, *Comput.*
402 *Geosci.*, 33, 538–562. DOI: 10.1016/j.cageo.2006.08.006, 2007.
- 403 Spada, G. and Melini, D.: SELEN4 (SELEN version 4.0): a Fortran program for solving the gravitationally
404 and topographically self-consistent sea-level equation in glacial isostatic adjustment modelling.
405 *Geoscientific Model Development*, 12, 5055–5075. DOI: 10.5194/gmd-12-5055-2019, 2019

- 406 [Su, S.W., Shang, Z.W., Wang, F., Wang, H.: Holocene Chenier: spatial and temporal distribution and sea](#)
407 [level indicators in Bohai Bay. Geological Bulletin of China, 30\(9\), 1382–1395. DOI: 10.1007/s11589-011-](#)
408 [0776-4, 2011\(in Chinese with English abstract\).](#)
- 409 [Tian, L.Z., Chen, Y.P., Jiang, X.Y., Wang, F., Pei, Y.D., Chen, Y.S., Shang, Z.W., Li, J.F., Li, Y., Wang, H.:](#)
410 [Post-glacial sequence and sedimentation in the western Bohai Sea, China. Marine Geology, 388m 12–24.](#)
411 [http://dx.doi.org/10.1016/j.margeo.2017.04.006, 2017.](#)
- 412 Tegmark, M.: An icosahedron-based method for pixelizing the celestial sphere, *Astrophys. J.*, 470, L81–L85,
413 <https://doi.org/10.1086/310310>, 1996.
- 414 Wang, F., Li, J.F., Chen, Y.S., Fang, J., Zong, Y.Q., Shang, Z.W., Wang H.: The record of mid-Holocene
415 maximum landward marine transgression in the west coast of Bohai Bay, China. *Marine Geology*, 359,
416 89–95. DOI: 10.1016/j.margeo.2014.11.013, 2015.
- 417 Wang, H., Chen, Y.S., Tian, L.Z., Li, J.F., Pei, Y.D., Wang, F., Shang, Z.W., Fan, C.F., Jiang, X.Y., Su,
418 S.W., Wang, H.: Holocene cheniers and oyster reefs in Bohai Bay: palaeoclimate and sea level changes.
419 *Geological Bulletin of China*, 30(9), 1405–1411. DOI: 10.1007/s11589-011-0776-4, 2011(in Chinese with
420 English abstract).
- 421 Wang, P.X., Min, Q.B. and Bian, Y.H.: Distributions of foraminifera and ostracoda in bottom sediments of
422 the northwestern part of the South Huanghai (Yellow) Sea and its geological significance. In: Wang, P.
423 (Eds.), *Marine Micropaleontology of China*. China Ocean Press, Beijing, pp. 93–114, 1985 (in Chinese
424 with English abstract).
- 425 Wang, P.X., Min, Q.B., Bian, Y.H., Cheng, X.R.: Strata of quaternary transgressions in east China: a
426 preliminary study. *Acta Geologica Sinica*, 1, 1–13. DOI: 10.1007/BF01077538, 1981 (in Chinese with
427 English abstract).
- 428 [Wang, Q. and Li F.L.: The changes of marine-continental conditions in the west coast of the Bohai Gulf](#)
429 [during Quaternary. Marine Geology&Quaternary Geology, 4, 83–89. DOI: 10.16562/j.cnki.0256-](#)
430 [1492.1983.04.013, 1983 \(in Chinese with English abstract\).](#)

- 431 Wang, R.B., Zhou, W., Li, F.L., Wang, H., Yang, G.Y., Yao, Z.J., Kuang, S.J.: Tectonic subsidence and
432 prospect of ground subsidence control in Tianjin area. *Hydrogeology & Engineering Geology*, 5, 12–17.
433 DOI: 10.1007/BF02873153, 2003 (in Chinese with English abstract).
- 434 Wang, Y.: The shell coast ridges and the old coastlines of the west coast of the Bohai Bay. *Bulletin of*
435 *Nanjing University (Edition of Natural Sciences)*, 8(3), 424–440. DOI: CNKI:SUN:NJDZ.0.1964-03-007,
436 1964 (with three plates) (in Chinese with English abstract).
- 437 [Wang, Y.M.: A preliminary study on the Holocene transgression on the coastal plain along the north-western](#)
438 [Bohai Bay. *Geographical Research*, 1\(2\), 59–69. DOI: 10.11821/yj1982020007, 1982 \(in Chinese with](#)
439 [English abstract\).](#)
- 440 Wang, Z., Zhuang, C., Staito, Y., Chen, J., Zhan, Q., Wang, X.: Early mid-Holocene sea-level change and
441 coastal environmental response on the southern Yangtze delta plain, China: implications for the rise of
442 Neolithic culture. *Quaternary Science Reviews*, 35, 51–62. DOI: 10.1016/j.quascirev.2012.01.005, 2012.
- 443 Wang, Z., Jones, B.G., Chen, T., Zhao, B., Zhan, Q.: A raised OIS3 sea level recorded in coastal sediments,
444 southern Changjiang delta plain, China. *Quaternary Research*, 79, 424–438. DOI:
445 10.1016/j.yqres.2013.03.002, 2013.
- 446 Xiong, H., Zong, Y., Qian, P., Huang, G., Fu, S.: Holocene sea-level history of the northern coast of South
447 China Sea. *Quaternary Science Reviews* 194, 12–26. <https://doi.org/10.1016/j.quascirev.2018.06.022>,
448 2018.
- 449 [Xiong, H., Zong, Y., Li, T., Long, T., Huang, G., Fu, S.: Coastal GIA processes revealed by the early to](#)
450 [middle Holocene sea-level history of east China. *Quaternary Science Reviews*, 233, 106249. DOI:](#)
451 [10.1016/j.quascirev.2020.106249, 2020.](#)
- 452 [Xue, C.T.: Historical changes in the Yellow River delta, China. *Marine Geology* 113, 321–329. DOI :](#)
453 [10.1016/0025-3227\(93\)90025-Q, 1993.](#)
- 454 [Yang, H.R. and Chen, Q.X.: Quaternary transgressions, eustatic changes and shifting of shoreline in east](#)
455 [China. *Marine Geology & Quaternary Geology*, 5\(4\), 69–80. DOI: 10.16562/j.cnki.0256-](#)
456 [1492.1985.04.011, 1985 \(in Chinese with English abstract\).](#)

- 457 [Zhang, Y.C., Hu, J.J. and Liu, C.F.: Preliminary recognition of sea and land changes along the east coast of](#)
458 [China since the terminal Pleistocene. Bulletin of the Chinese Academy of Geological Sciences, 19, 37–52.](#)
459 <https://www.ixueshu.com/document/8e1a59a8c6fd86ca318947a18e7f9386.html>, 1989 (in Chinese with
460 [English abstract\).](#)
- 461 [Zhao, S.L., Yang, G.F., Cang, S.X., Zhang, H.C., Huang, Q.F., Xia, D.X., Wang, Y.J., Liu, F.S., Liu, C.F.:](#)
462 [On the marine stratigraphy and coastlines of the western coast of the gulf of Bohai. Oceanologia Et](#)
463 [Limnologia Sinica, 9\(1\), 15–25](#)
464 [ar_id=1978, 1978 \(in Chinese with English abstract\).](http://qdhs.ijournal.cn/hyyhz/ch/reader/create_pdf.aspx?file_no=19780102&flag=&journal_id=hyyhz&ye)
- 466 [Zhao, X.T., Geng, X.S., Zhang, J.W.: Sea level changes of the eastern China during the past 20000 years.](#)
467 [Acta Oceanologia Sinica, 1\(2\), 269–281.](#)
468 [alg=1, 1979.](http://www.hyxb.org.cn/aos/ch/reader/create_pdf.aspx?file_no=19790208&year_id=1979&quarter_id=2&f)
- 470 [Zong, Y.: Mid-Holocene sea-level highstand along the southeast coast of China. Quaternary International,](#)
471 [117, 55–67. DOI: 10.1016/S1040-6128\(03\)00116-2, 2004.](#)

472

Table 1. Analytical data used to establish SLIPs.

Beta-lab code	Depth (m)	Altitude (m, msl)	Dated material	$\delta^{13}\text{C}$ (‰)	Conventional age (BP)	Calibrated age (BP) (2 σ)	Median age (BP)	Indicative meaning and range	Sediment compaction (m)*	Palaeo-mean sea level
Core DC01										
329636	8.40	-4.66	Peat	-26.8	6950 \pm 40	7523-7430	7487	Terrestrial peat		
329637	9.27	-5.53	Bulk organic	-18.2	7410 \pm 60	8372-8153	8248	Terrestrial peat		
Core QX01										
329647	5.52	+0.36	Bulk organic	-22.5	4300 \pm 30	4892-4829	4343**	1.78 \pm 0.53	0.29 \pm 0.04	-1.14 \pm 0.57
329644	6.35	-1.19	Bulk organic	-23.6	5010 \pm 50	5900-5644	5226**	1.78 \pm 0.53	0.30 \pm 0.04	-2.68 \pm 0.57
329643	7.20	-2.04	Bulk organic	-25.0	5090 \pm 30	5912-5748	5288**	1.78 \pm 0.53	0.25 \pm 0.03	-3.58 \pm 0.56
329641	8.20	-3.04	Peat	-24.6	5830 \pm 30	6732-6554	6647	1.78 \pm 0.53	0.24 \pm 0.03	-4.58 \pm 0.56
329642	8.70	-3.54	Peat	-24.3	6030 \pm 40	6981-6778	6875	1.78 \pm 0.53	0.21 \pm 0.03	-5.11 \pm 0.56
329645	9.16	-4.00	Peat	-27.4	6220 \pm 40	7250-7006	7117	1.78 \pm 0.53	0.18 \pm 0.02	-5.60 \pm 0.55
329640	11.39	-6.23	Peat	-25.3	7010 \pm 30	7935-7786	7855	1.78 \pm 0.53	0.01 \pm 0.01	-8.00 \pm 0.54
329646	13.05	-7.89	Peat	-25.1	7200 \pm 30	8057-7952	8002	Terrestrial peat		
Core QX03										
353792	2.91	1.47	Peat	-20.6	2350 \pm 30	2461-2326	2357	Terrestrial peat		
353794	4.90	-0.42	Peat	-24.0	3390 \pm 30	3699-3569	3634	1.78 \pm 0.53	0.16 \pm 0.02	-2.01 \pm 0.55
353796	7.39	-3.01	Plant material	NA	5930 \pm 30	6799-6671	6752	1.78 \pm 0.53	0.10 \pm 0.02	-4.68 \pm 0.55
353798	8.63	-4.25	Plant material	-26.7	6410 \pm 40	7420-7271	7350	1.78 \pm 0.53	0.01 \pm 0.01	-6.02 \pm 0.54
353800	9.60	-5.22	Plant material	-28.2	6690 \pm 40	7622-7478	7562	Terrestrial peat		
353802	12.40	-8.02	Plant material	-28.3	7280 \pm 40	8429-8325	8397	Terrestrial peat		
Core QX02										

332798	3.65	-0.08	Bulk organic	-23.6	3680±30	4091-3913	3517**	1.78±0.53	0.30±0.04	-1.57±0.57
332792	5.68	-2.11	Bulk organic	-24.0	5450±30	6300-6204	5718**	1.78±0.53	0.36±0.04	-3.54±0.57
333329	7.27	-3.70	Peat	-26.7	6350±30	7331-7240	7283	1.78±0.53	0.32±0.04	-5.16±0.57
333330	8.98	-5.41	Peat	-26.3	6600±30	7522-7434	7494	1.78±0.53	0.19±0.02	-7.00±0.55
333331	10.97	-7.40	Peat	-27.2	7020±30	7934-7792	7867	Terrestrial peat		
333333	12.42	-8.85	Peat	-26.3	7140±40	8023-7925	7966	Terrestrial peat		
Core ZW15										
255821	1.6	0.03	Bulk organic	-22.5	2930±30	3168-2976	2584**	1.78±0.53	0.32±0.04	-1.44±0.57
356208	12.6	-10.97	Plant material	-25.0	7450±40	8358-8186	8271	1.78±0.53	0.00	-12.75±0.53
356209	13.5	-11.87	Plant material	-25.5	7640±40	8521-8381	8430	Terrestrial peat		
Core Q7										
358054	1.3	2.16	Bulk organic	-20.4	530±30	559-510	540	1.78±0.53	0.10±0.02	+0.49±0.55
357153	17.2	-13.74	Plant material	-28.0	7990±40	9005-8705	8868	1.78±0.53	0.16±0.02	-15.36±0.55
357157	18.85	-15.39	Bulk organic	-24.6	9140±40	10411-10226	9718**	1.78±0.53	0.00	-17.18±0.53
Core CZ01										
395014	15.42	-8.53	Peat	-27.5	8930±40	10099-9914	10047	Terrestrial peat		
Core CZ02										
395022	12.19	-6.42	Peat	-23.1	7950±30	8980-8648	8830	Terrestrial peat		
Core CZ03										
395026	4.42	-0.48	Bulk organic	-24.2	2730±30	2877-2762	2325**	1.78±0.53	0.12±0.02	-2.15±0.55
395027	6.15	-2.21	Peat	-25.1	4790±30	5593-5470	5517	1.78±0.53	0.19±0.02	-3.80±0.55
395028	6.54	-2.57	Bulk organic	-27.1	5830±30	6732-6554	6114**	1.78±0.53	0.18±0.03	-4.18±0.56
395029	7.51	-3.54	Peat	-26.7	6230±30	7251-7019	7167	1.78±0.53	0.14±0.02	-5.19±0.55
395030	9.22	-5.25	Peat	-27.3	6640±30	7576-7468	7528	1.78±0.53	0.01±0.01	-7.03±0.54

395031	9.34	-5.37	Peat	-20.0	6660±30	7583-7483	7535	1.78±0.53	0.00	-7.15±0.53
395032	10.23	-6.26	Peat	-27.2	6900±30	7794-7669	7726	Terrestrial peat		
395034	12.4	-8.43	Peat	-27.2	7290±30	8171-8025	8102	Terrestrial peat		
Core CZ87										
403413	2.66	1.8	Bulk organic	-20.8	2420±30	2696-2351	2446	Terrestrial peat		
403414	4.51	-0.05	Bulk organic	-23.8	3330±30	3637-3477	3566	Terrestrial peat		
406826	5.75	-1.29	Bulk organic	-24.1	4020±30	4536-4420	3970**	1.78±0.53	0.25±0.03	-2.83±0.56
403417	11.05	-6.59	Plant material	-27.9	6300±30	7275-7165	7223	1.78±0.53	0.04±0.01	-8.33±0.54
403418	12.62	-8.16	Plant material	-27.6	6990±30	7876-7736	7829	Terrestrial peat		
Core CZ61										
407339	2.52	1.24	Bulk organic	-20.8	2310±30	2359-2306	2337	Terrestrial peat		
406823	4.72	-0.96	Plant material	NA	2780±30	2952-2793	2877	1.78±0.53	0.16±0.02	-2.58±0.55
406824	6.20	-2.44	Bulk organic	-23.9	6100±30	7029-6884	6433**	1.78±0.53	0.25±0.03	-3.98±0.56
403397	9.73	-5.97	Plant material	-19.6	6760±30	7664-7577	7615	1.78±0.53	0.00	-7.75±0.53
403398	11.04	-7.37	Plant material	-27.5	7000±30	7932-7756	7842	Terrestrial peat		
403399	12.90	-9.14	Plant material	-28.0	7160±30	8018-7939	7980	Terrestrial peat		
Core CZ65										
399705	4.93	-1.97	Bulk organic	-18.5	3920±30	4428-4280	3397	Terrestrial peat		
399708	9.58	-6.62	Plant material	-27.2	7000±30	7883-7756	7823	1.78±0.53	0.01±0.01	-8.39±0.54
399710	11.50	-8.54	Plant material	-27.1	7250±30	8162-8001	8080	Terrestrial peat		
Core CZ80										
403401	3.73	2.69	Bulk organic	-20.3	3170±30	3452-3346	3400	Terrestrial peat		
403403	6.57	-0.15	Bulk organic	-22.1	5050±30	5901-5726	5298	1.78±0.53	0.20±0.03	-1.74±0.56
406825	8.75	-2.33	Peat	NA	5840±30	6736-6562	6660	1.78±0.53	0.09±0.01	-4.02±0.54

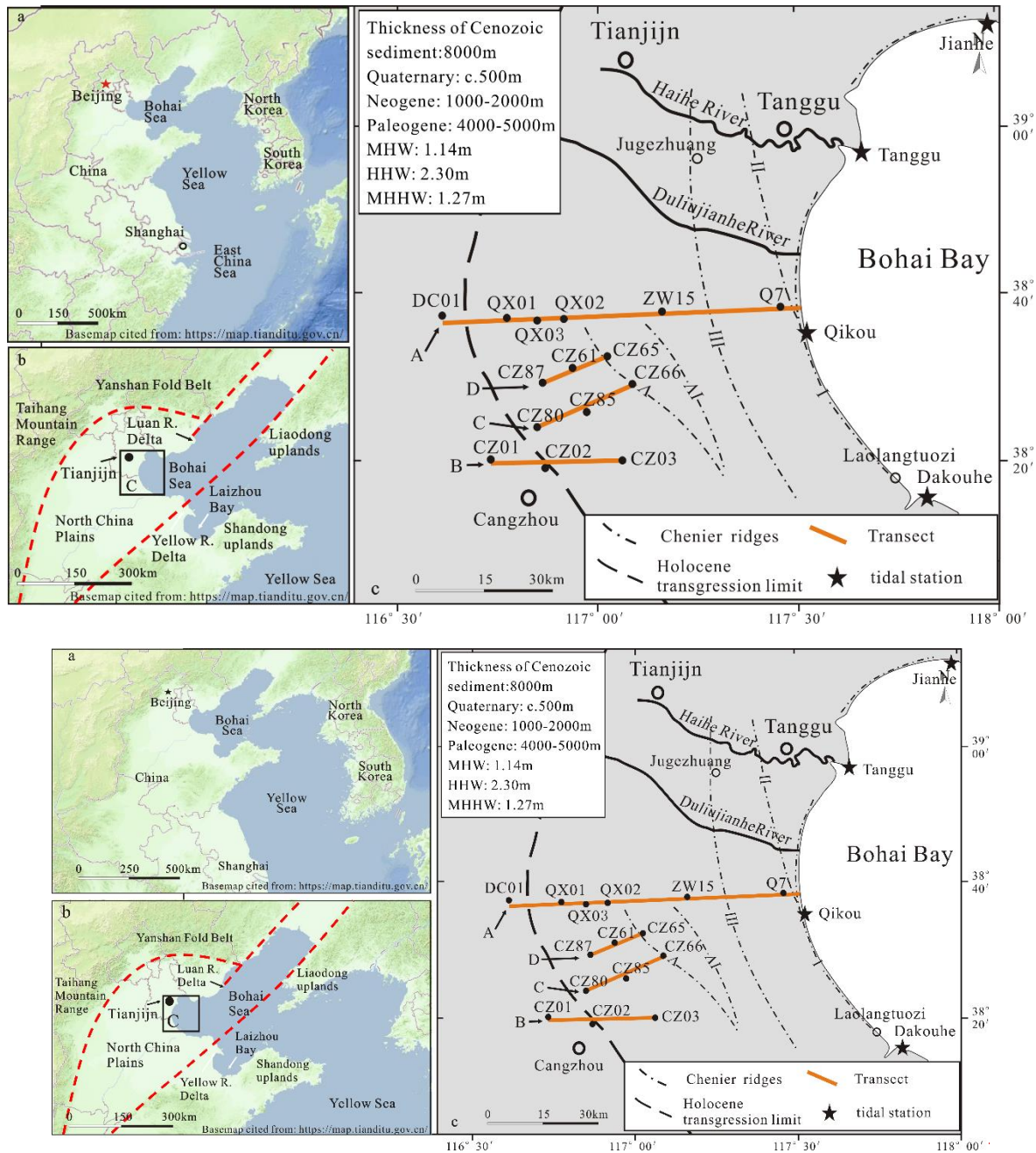
403408	11.53	-5.11	Plant material	-27.5	6450±30	7428-7313	7370	Terrestrial peat		
403409	12.05	-5.63	Plant material	-27.9	6610±30	7565-7440	7503	Terrestrial peat		
403410	12.34	-5.92	Plant material	-26.4	6860±30	7759-7618	7687	Terrestrial peat		
403411	13.84	-7.42	Plant material	-24.6	7300±30	8175-8029	8105	Terrestrial peat		
Core CZ85										
399719	3.67	0.94	Bulk organic	-20.5	3460±30	3671-3641	3225**	1.78±0.53	0.17±0.03	-0.68±0.56
399720	6.77	-2.16	Bulk organic	-25.4	5830±30	6732-6554	6114**	1.78±0.53	0.08±0.01	-3.87±0.54
399721	8.33	-3.72	Plant material	-26.4	6020±30	6947-6785	6862	1.78±0.53	0.01±0.01	-5.49±0.54
399722	12.70	-8.09	Plant material	-28.0	7270±30	8165-8015	8096	Terrestrial peat		
Core CZ66										
399712	3.62	0.25	Bulk organic	-23.4	3930±30	4440-4282	3856**	1.78±0.53	0.32±0.04	-1.22±0.57
399713	5.21	-1.34	Bulk organic	-25.1	5730±30	6632-6445	5992**	1.78±0.53	0.39±0.05	-2.74±0.58
399714	8.14	-4.27	Plant material	-27.4	6710±30	7651-7510	7581	1.78±0.53	0.24±0.03	-5.81±0.56
399715	10.03	-6.16	Plant material	-26.6	6790±30	7675-7587	7635	1.78±0.53	0.08±0.01	-7.86±0.54
399716	12.49	-8.62	Plant material	-27.1	7220±30	8156-7965	8021	Terrestrial peat		
399718	13.63	-9.76	Plant material	-27.6	7670±30	8523-8406	8452	Terrestrial peat		

473 s* Sediment compaction = 10% of compressible thickness divided by lapse time of deposition in the past 9000 years

474 ** corrected for marine influence on salt marsh organic sample fraction ages of peaty clay

475

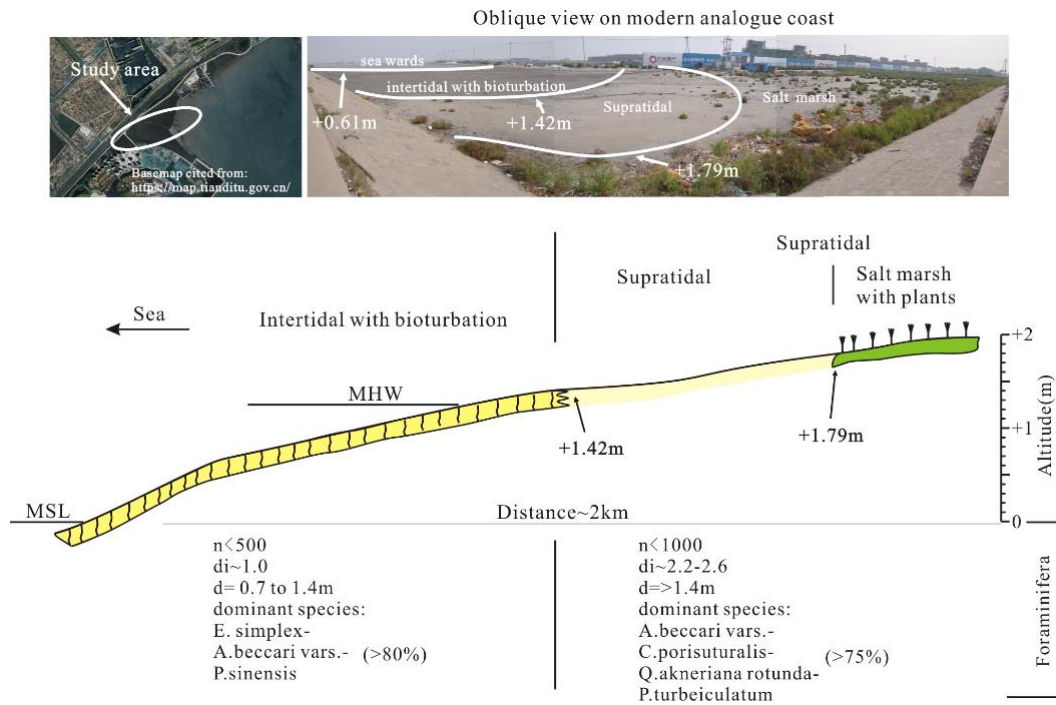
476 Figure captions



477

478

479 Figure 1. The study area; (a) location of Bohai Bay and Yellow Sea; (b) location of the study area and major river
 480 deltas; red dashed lines indicate the topographic boundaries of coastal lowland, (c) locations of boreholes,
 481 transects A, B, C, D, Chenier ridges (Su et al. (2011; Wang et al., 2011) and Holocene transgression limit (Xue,
 482 1993). The basemap of Fig.1a and Fig.1b are cited from "map world" (<https://www.tianditu.gov.cn/>, National
 483 Platform for Common Geospatial Information Services, China)

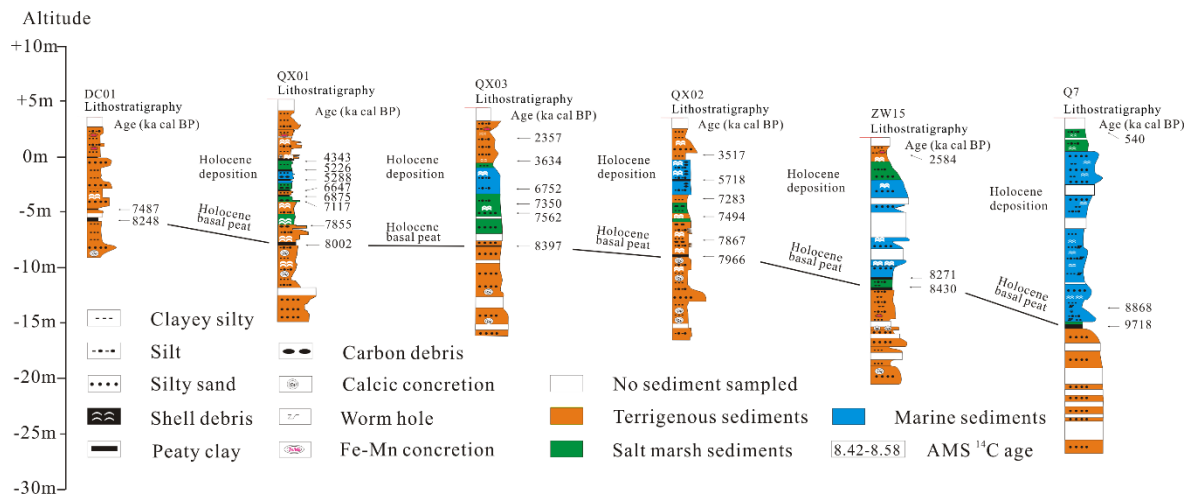


484

485 **Figure 2. Schematic cross-section of the modern tidal flat of the study area showing two characteristic**

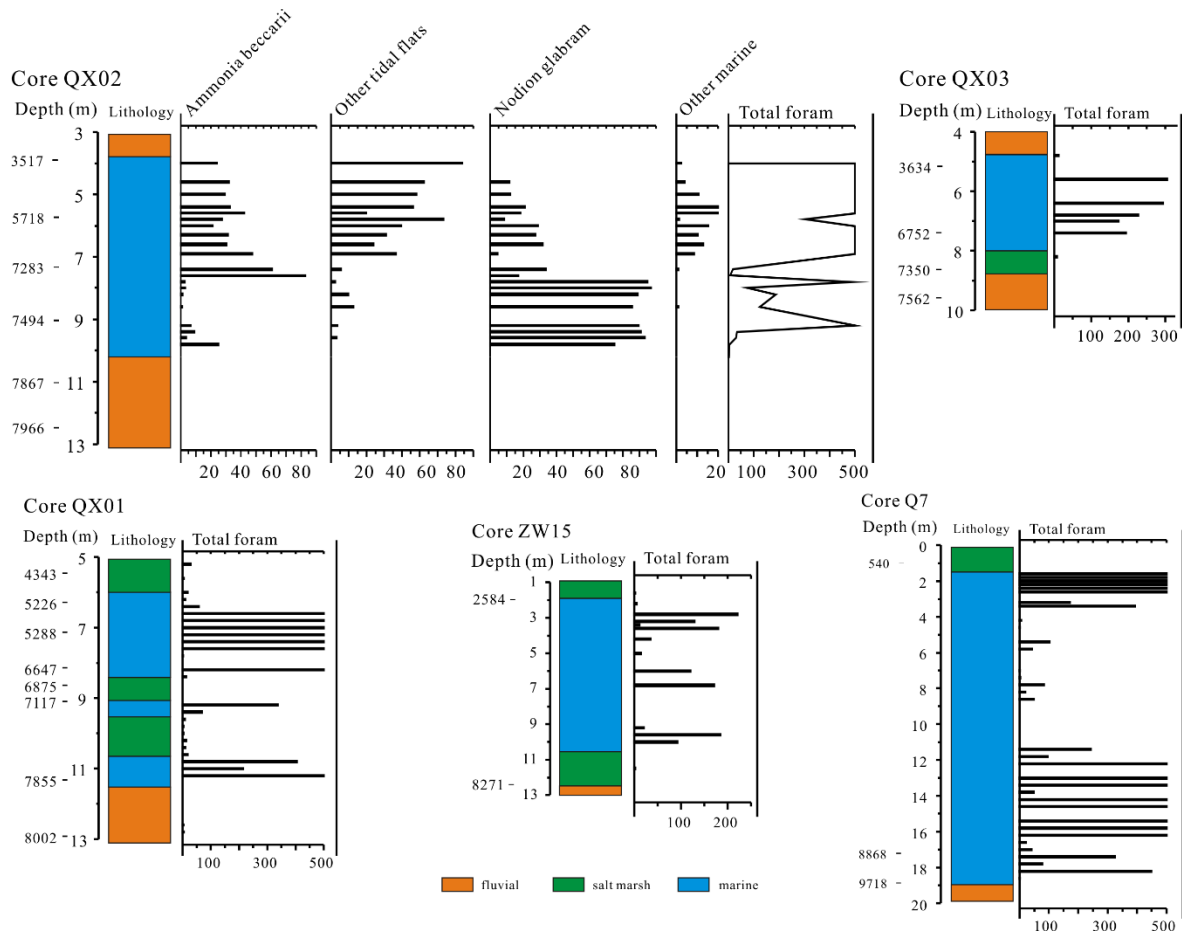
486 **foraminiferal zones. The basemap of study area is cited derived from "map world" (<https://www.tianditu.gov.cn/>,**

487 **National Platform for Common Geospatial Information Services, China)**



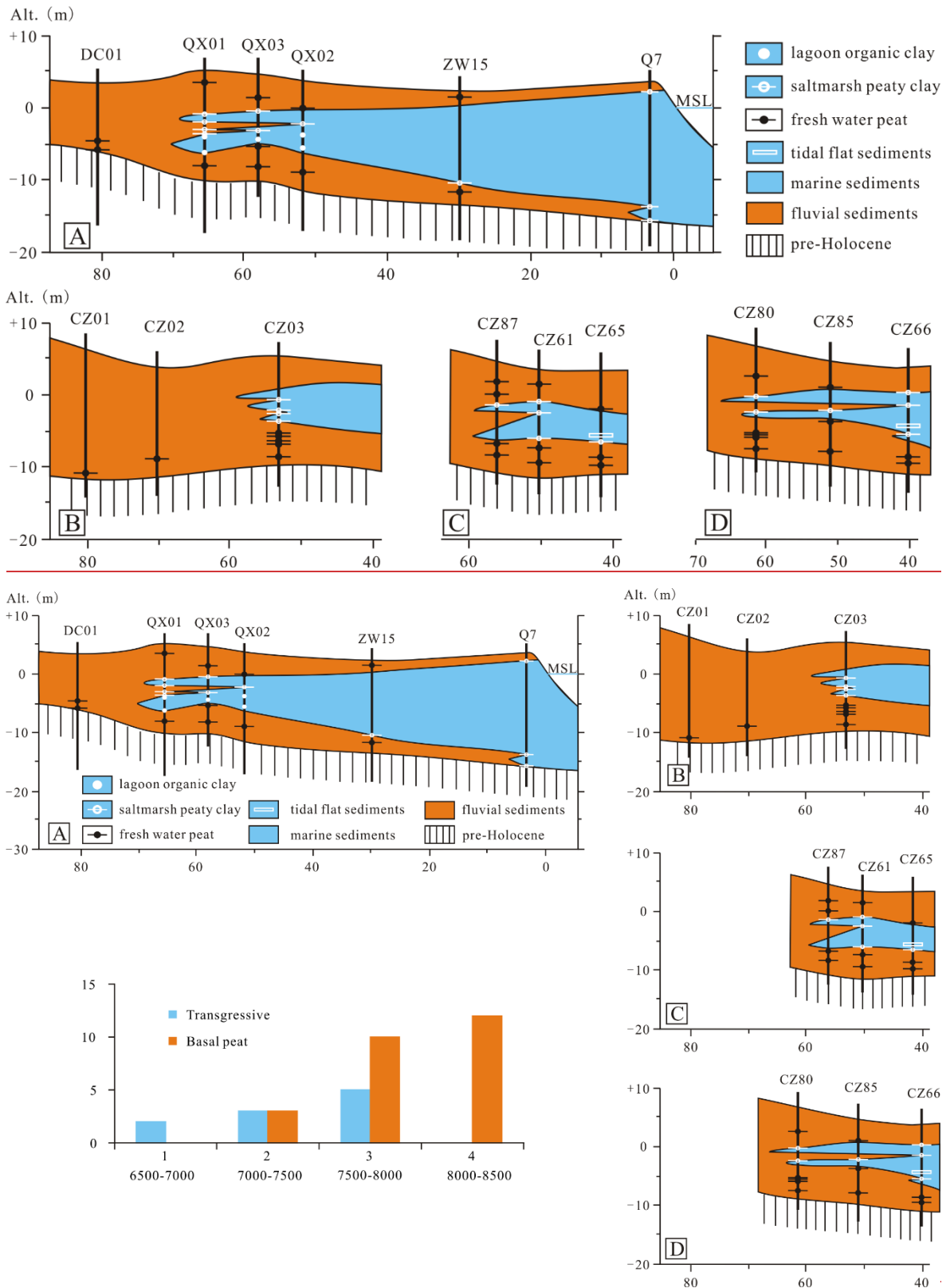
488

489 **Figure 3. The lithostratigraphy of transect A, with details of dated sedimentary horizons.**



490

491 **Figure 4. Foraminiferal counts from five cores of transect A. Counts > 500 are shown as 500.**

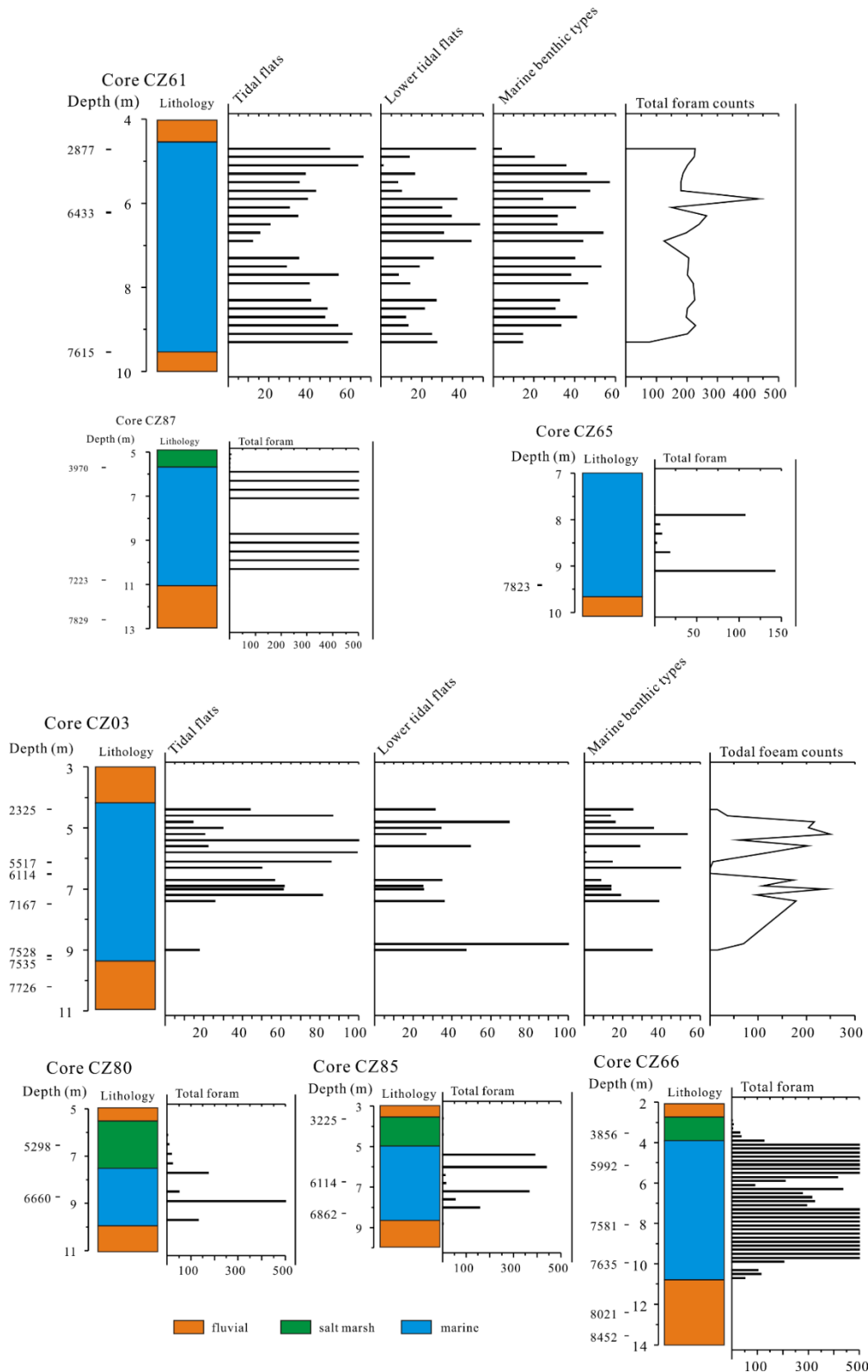


492

493

494

Figure 5. The lithostratigraphy of transects B, C and D, with details of dated sedimentary horizons.



495

496 **Figure 6. Foraminiferal counts from five cores of transects B, C and D. Counts > 500 foraminifera are shown as**

497 **500.**

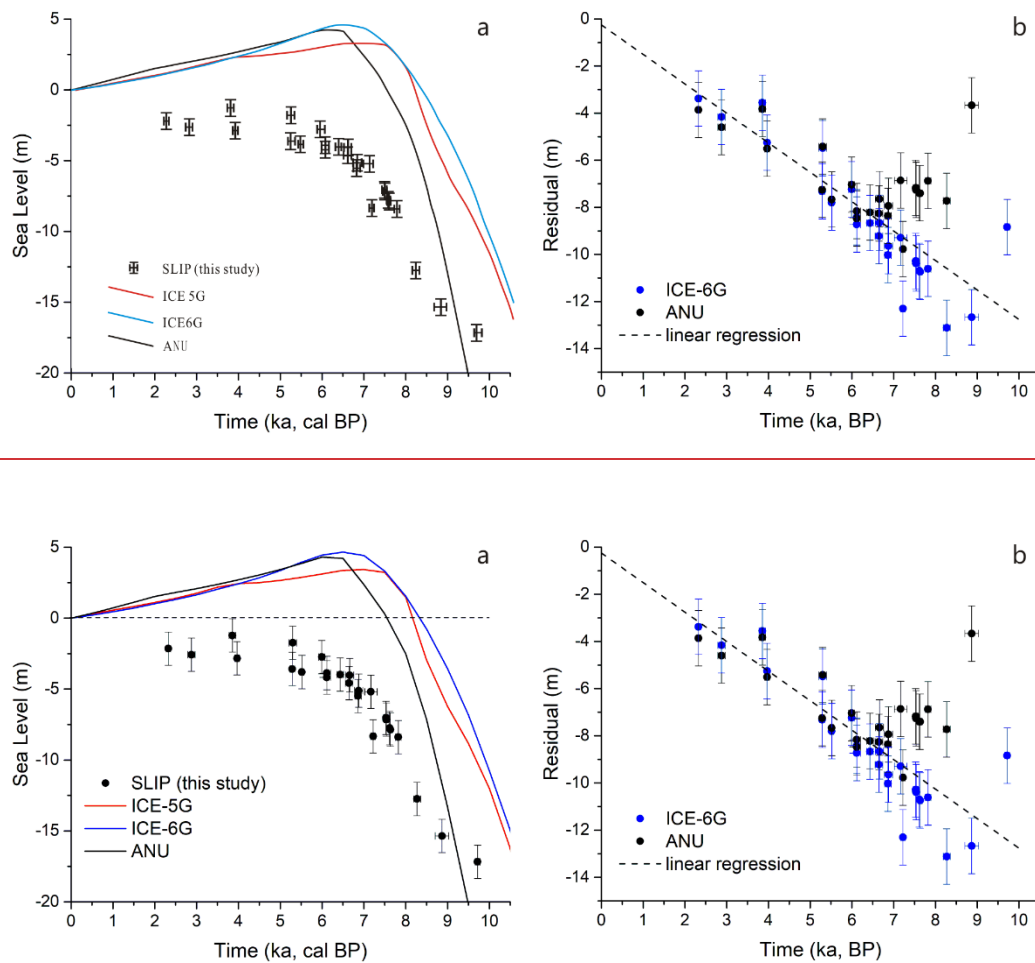


Figure 7. Observed and predicted sea level in Bohai Bay and resulting residuals; (a) SLIPs generated in this study and sea-level predictions. ICE-5G, ICE-6G and ANU are ice-GIA models described in section 3.6. Lithospheric thickness (km): 65 (ANU), 90 (5G and 6G); upper mantle viscosity (Pa s) = 0.5×10^{21} (ANU, 5G, 6G); lower mantle viscosity (Pa s): 10×10^{21} (ANU), 2.7×10^{21} (5G), 3.2×10^{21} (6G); see also Table S1; age error bars are too small to be clearly visible. (b) Sea-level residuals plotted against time. Residuals are the difference between SLIPs and interpolated model data points. Error bars are derived from SLIP uncertainties. The trend line (dashed line) is computed as a least-squares regression on the mean residuals obtained with ANU and ICE-6G. The regression line approximates zero elevation remarkably closely which gives confidence that the calculated 1.25 mm/a for the non-GIA component is correct.

510 Author contribution

Author name	Contributions
Fu Wang	Scientific questions choice, location choice of the boreholes <u>design of field work including</u> , sampling and , <u>measurements</u> , data analyses, results and discussion, paper writing and revising.
Yongqiang Zong	Revise part of the paper and English writing check.
Barbara Mauz	Revise part of the paper and English writing check.
Jianfen Li	Sampling and foraminifera analysis <u>ise</u> .
Jing Fang	Sampling and foraminifera analysis <u>ise</u> .
Lizhu Tian	Sampling and foraminifera analysis <u>ise</u> .
Yongsheng Chen	Sampling and foraminifera analysis <u>ise</u> .
Zhiwen Shang	Sampling and foraminifera analysis <u>ise</u> .
Xingyu Jiang	Sampling and foraminifera analysis <u>ise</u> .
Giorgio Spada	<u>GIA model work Modelling sea level part “3.6” and “5.3”</u> and writing sec 3.6
Daniele Melini	<u>GIA model work and residual calculation</u> Modelling sea level part “3.6” and “5.3”

511